



UNIVERSITY OF LEEDS

This is a repository copy of *Binary alkali-activated systems obtained by the valorisation of calcined kaolin sludge and bottom ash*.

White Rose Research Online URL for this paper:

<https://eprints.whiterose.ac.uk/192314/>

Version: Accepted Version

---

**Article:**

Longhi, MA, Rodríguez, ED, Bernal, SA [orcid.org/0000-0002-9647-3106](https://orcid.org/0000-0002-9647-3106) et al. (2 more authors) (2022) Binary alkali-activated systems obtained by the valorisation of calcined kaolin sludge and bottom ash. *Advances in Cement Research*, 34 (2). pp. 67-79. ISSN 0951-7197

<https://doi.org/10.1680/jadcr.20.00098>

---

© 2021 ICE Publishing. This is an author-produced version of a paper subsequently published in *Advances in Cement Research*. Uploaded in accordance with the publisher's self-archiving policy.

**Reuse**

Items deposited in White Rose Research Online are protected by copyright, with all rights reserved unless indicated otherwise. They may be downloaded and/or printed for private study, or other acts as permitted by national copyright laws. The publisher or other rights holders may allow further reproduction and re-use of the full text version. This is indicated by the licence information on the White Rose Research Online record for the item.

**Takedown**

If you consider content in White Rose Research Online to be in breach of UK law, please notify us by emailing [eprints@whiterose.ac.uk](mailto:eprints@whiterose.ac.uk) including the URL of the record and the reason for the withdrawal request.



[eprints@whiterose.ac.uk](mailto:eprints@whiterose.ac.uk)  
<https://eprints.whiterose.ac.uk/>

# Binary alkali activated systems obtained by the valorisation of two industrial wastes

Márlon Longhi<sup>1</sup>; Erich D. Rodríguez<sup>2\*</sup>; Susan A. Bernal<sup>3,4</sup>; John L. Provis<sup>3</sup>; Ana Paula Kirchheim<sup>1</sup>.

ORCID of the authors:

0000-0002-6966-7888; 0000-0003-1914-4541; 0000-0002-9647-3106; 0000-0003-3372-8922; 0000-0002-8241-0331

<sup>1</sup> *Building Innovation Research Unit, Universidade Federal do Rio Grande do Sul (NORIE/UFRGS), Porto Alegre, RS Brazil*

<sup>2</sup> *Department of Structures and Civil Construction. Center of Technology, Universidade Federal de Santa Maria (CT/UFSM), Santa Maria, RS, Brazil.*

<sup>3</sup> *Department of Materials Science and Engineering, The University of Sheffield, Sheffield S1 3JD, United Kingdom.*

<sup>4</sup> *School of Civil Engineering, The University of Leeds, Leeds LS2 9JT, United Kingdom*

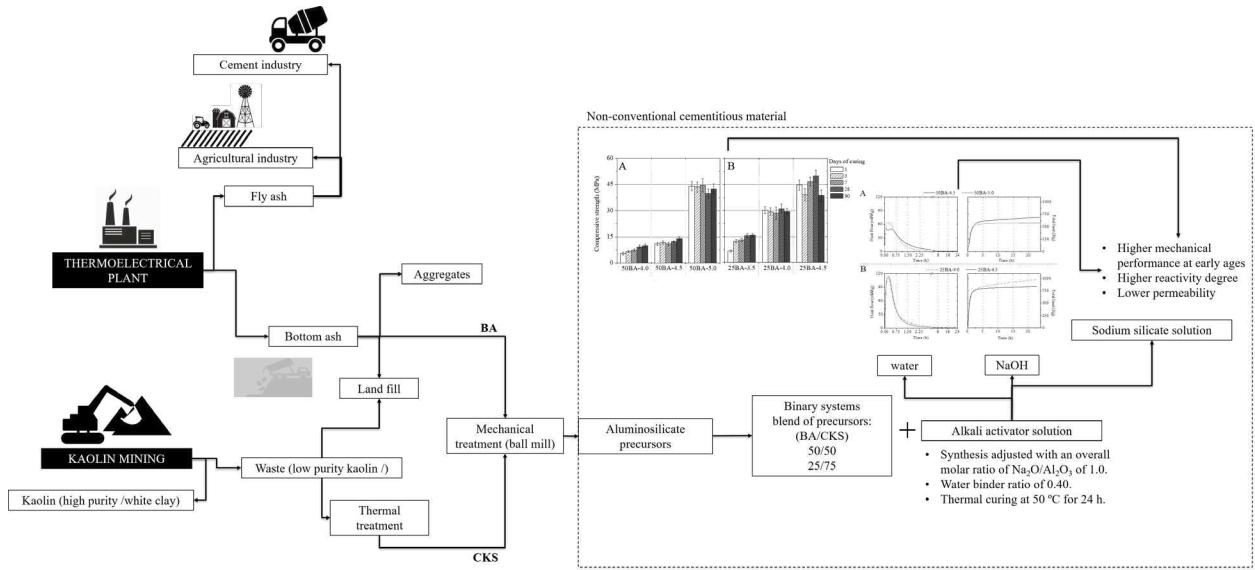
Corresponding author: marlonlonghi@gmail.com

## Abstract

This paper assesses the use and potential valorisation of two industrial wastes generated at large scale in Brazil, which are currently disposed in landfills, as raw materials for the production of geopolymers. Specifically, a kaolinitic sludge from the mining industry (CKS), and a bottom ash (BA) generated during coal combustion in a thermal power station, were used as aluminosilicate precursors in geopolymer synthesis. The geopolymers were synthesised at 50 °C, with a Na<sub>2</sub>O/Al<sub>2</sub>O<sub>3</sub> molar ratio of 1.0, and different SiO<sub>2</sub>/Al<sub>2</sub>O<sub>3</sub> molar ratios adjusted by the different mix proportions between precursors and by manipulating the content of the soluble silicate solution used as the activator. The mechanical strength and reaction products formed during the geopolymerisation process were assessed up to 90 days of curing by compressive strength and the assessment of some microstructural features. To understand the behaviour of these materials in use and to correlate this to microstructural properties, mortar samples were produced and assessed for compressive strength, flexural strength and water sorption by capillarity. The use of CKS as the main component of the precursor blend provides a geopolymer with better mechanical properties due to its higher reactivity, when compared to the BA. The content of soluble silicates in the alkali activator plays an important role during geopolymerisation, improving the mechanical properties due to formation of a more cross-linked and denser structure. The mortars show a compressive strength higher than 55 MPa after 28 days and low water absorption by capillarity, which is associated with a refined pore structure. This elucidates the feasibility of valorising these industrial residues as precursors for geopolymer cements when the mix proportion and synthesis conditions are adjusted and optimised.

*Keywords: Bottom ash, calcinated kaolin sludge, geopolymers, waste valorisation.*

45 **Graphical abstract**



46

47 **Statement of novelty**

48 This research was undertaken in order to assess the potential use of two industrial wastes, including: a calcined  
 49 kaolinitic sludge (from the mining industry) and bottom ash (from a thermoelectrical industry) as precursors to  
 50 produce geopolymers. This valorisation reduces the environmental damage associated with generating enormous  
 51 quantities of these materials and their current disposition in landfill. The materials have different physicochemical  
 52 properties, as well as reactivity, which influences the mechanical and microstructural properties of the geopolymer  
 53 formed. The high reactivity of the kaolinitic precursor provides higher strength but requires a large amount of  
 54 activator, on the other way, the inclusion of bottom ash, which has lower reactivity reduce the mechanical  
 55 performance. The use of these materials as precursors for geopolymers gives value to non-valorised wastes.

56

## 57 1. Introduction

58 National and international regulations and policies, and increasing recognition of the need to live sustainably across  
59 all sectors of society, have promoted interest in decreasing the total volume of waste produced and thus to improve  
60 the sustainability of solid waste management in the industrial sector. Therefore, there is a strong move toward  
61 viewing waste as a resource that can be recycled and recovered. The valorisation of industrial wastes through re-use,  
62 recycling, or energy recovery has a significant environmental, economic and social benefit due to the reduction of  
63 areas used for landfill disposal, reduction of pollution caused by the contamination of soil, ground water and  
64 greenhouse gas emissions, reduction of consumption of fossil fuels, as well as the generation of new jobs. Although  
65 solid waste management was not included explicitly in the Millennium Development Goals (MDGs) and their  
66 indicators [1], there nonetheless exists a clear link, where better and more efficient waste management offer better  
67 opportunities for income generation.

68  
69 The present article demonstrates the potential for valorisation of two different wastes generated by a power station  
70 plant and by the mining of kaolin, which are currently disposed in landfill without any added value. The first residue  
71 assessed here is a product generated by the combustion of coal in a power station plant. Coal combustion produces  
72 ~40% of global electricity and it is estimated that more than 778 Mt/y of wastes and by-products are generated [2,  
73 3]. However, the environmental impact of coal ashes when disposed in landfills is becoming more widely known.  
74 The erosion, dispersal, leaching, and atmospheric transport of the ashes may spread contaminants into natural  
75 aquatic and terrestrial systems, causing water and soil contamination, biodiversity loss, and environmental  
76 degradation [4–7]. Recycling of coal ashes can be a feasible alternative to disposal with significant economic and  
77 environmental benefits.

78  
79 Among the various different coal combustion by-products (CCPs), fly ash (FA) can be considered the most  
80 important due to its importance within the cement production market, considering its physicochemical features and  
81 the large quantities generated (~80% of total CCPs). Bottom ash (BA), which is the second most important CCP, is  
82 defined as the larger and heavier particles that are accumulated in the bottom of the boiler or furnace during coal  
83 combustion. BA has a low rate of reuse as a value-added by-product (46% and 39% in the EU and the US,  
84 respectively) [8, 9]. The BA that is not suitable for the cement industry (in blended cements or as a feed for clinker  
85 production) and then can be used as structural fill, in mining applications, as a road sub-base, or in snow and ice  
86 controller [10, 11]. Taking into account the large volume of this material that is currently disposed in landfill, and  
87 the new regulations requiring its safer disposal [12], BA management has become an economical and environmental  
88 concern for electricity generators. In the search for a more efficient pathway to reuse, BA has been also assessed as  
89 a mineral admixture in Portland-blended cements, and its pozzolanic reactivity can be improved through mechanical  
90 treatment for size reduction [13]. However, the generally low reactivity, low density, and high porosity of BA have  
91 been the main barriers to its use as a supplementary cementitious material (SCM).

92  
93 There do exist some reports related to the use of BA as a raw material for the production of non-conventional  
94 cementitious binders, including alkali-activated cements or geopolymers [14–18]. Geopolymers are a type of cement  
95 produced by chemical activation of an aluminosilicate precursor by a highly alkaline reagent in order to obtain a  
96 material with cementitious properties. Geopolymers are often described as offering low energy consumption and  
97 low CO<sub>2</sub> emissions when compared with Portland cement, while enabling valorisation of high-volume industrial  
98 wastes or by-products [19, 20]. The relatively low reactivity of BA can yield geopolymers with lower mechanical  
99 performance than those based on FA [15]. However, the performance of BA-based systems can be improved  
100 through the application of mechanical treatment [18], and/or the inclusion of a secondary precursor with higher  
101 reactivity [21].

102  
103 Taking into account the low reactivity of the BA used in this study [22–24], a waste derived from the kaolin mining  
104 industry was assessed as a secondary precursor: a rejected kaolinitic clay sludge, which is generated during the  
105 whitening and adjustment of the particle size distribution in wet processes for kaolin purification. Brazil is now the  
106 fifth-largest global producer of kaolin, reaching almost 2 Mt/year [25], which leads to generation of ~0.5 Mt/year of  
107 kaolin sludge and with a stockpile of approximately 10 Mt [26]. This residue is classified as an inorganic and inert  
108 material, class II, according to the Brazilian standards [27], and a non-hazardous material by the U.S. Environmental  
109 Protection Agency (EPA). In its production, kaolin is dispersed in water and screened for removal of coarser  
110 particles (> 44 μm). The slurry thus obtained is centrifuged to separate the kaolin into particle size fractions, which  
111 are then whitened. Finally, the kaolin is dewatered by filtration and then dried. The mineral matter rejected is in the  
112 form of a coarse-grained kaolin sludge, which is mainly disposed in large artificial basins [28, 29].

113  
114 The sludge contains mainly kaolinite, with some of quartz and anatase [26]. This high content of kaolinite offers the  
115 potential for valuable use after its controlled thermal treatment, where a material with high pozzolanic reactivity and

high reactivity degree can be obtained [30–32]. The high content of SiO<sub>2</sub> and Al<sub>2</sub>O<sub>3</sub>, as well as the high reactivity of the calcined kaolin sludge (CKS), highlights a potential alternative route for its reuse as a raw material for the production of alkali-activated cements [33, 34]. Although commercial metakaolin (MK) has been one of the most used aluminosilicate precursors in geopolymer synthesis, the high cost of high purity kaolinite clays represents a barrier to large-scale production of MK geopolymer-based products [19].

In this way, the correct mix proportions between this two industrial wastes and activator can allow the use of these materials as precursors to produce geopolymers. The CKS requires a high-water consumption due its particles plate-shape morphology, however presents higher reactivity. The thermal treatment of the kaolin sludge, which is done in order to increase its reactivity, contributes significantly to its cost production due to the energy involved to achieve temperatures close to 700 °C. On the other hand, even though the BA exhibits lower reactivity; its high stock (or availability) and considering that high temperature treatments are not required, elucidates its potential for its valorisation. As these materials present specific properties, it is necessary to understand some microstructural features and mechanical properties to evaluate their performance as precursors for the synthesis of blended alkali-activated-type binders. In this sense, the development of non-conventional cements offers alternative pathways for the valorisation of kaolin mining wastes and bottom ash, which are available in large volumes and currently landfilled.

This paper assesses the use of these two industrial wastes for producing binary geopolymers based on different BA/CKS blends and mix design parameters. The chemistry and microstructural features of the reaction products formed were assessed through isothermal calorimetry (IC), thermogravimetric analysis (TGA), X-ray diffractometry (XRD) and Fourier transformed infrared spectroscopy (FTIR), in conjunction with determination of compressive strength and mass transport properties.

## 2. Experimental programme

### 2.1. Materials

A bottom ash from a coal power station in Triunfo (RS), Brazil, and a waste kaolin sludge derived from the kaolin mining industry from Pará (Brazil), were used in this study. The bottom ash was sieved to 100% passing 300 µm, and then ball milled for 1 h. The final material showed a mean particle size of 17.4 µm with a d<sub>90</sub> of 36.4 µm and a specific surface area, determined by the Brunauer-Emmett-Teller (BET) method, of 5.21 m<sup>2</sup>/g. The kaolin sludge was calcined at 750 °C for 1 h and then milled in a ball mill for 1 h. The calcined kaolin sludge (CKS) exhibited a mean particle size of 11.0 µm and a BET specific surface area of 19.7 m<sup>2</sup>/g. The chemical compositions of the aluminosilicate sources are shown in Table 1. The higher specific surface of the CKS is related to the presence of layered particles, when compared to the BA.

Table 1. Chemical composition of raw materials, as determined by X-ray fluorescence.

	Bottom ash (CP)	Calcined kaolin sludge (CKS)
SiO <sub>2</sub>	62.9	59.5
Al <sub>2</sub> O <sub>3</sub>	18.2	32.9
Fe <sub>2</sub> O <sub>3</sub>	9.0	2.7
K <sub>2</sub> O	2.0	0.1
MgO	0.2	-
MnO	0.1	-
TiO <sub>2</sub>	1.7	2.0
P <sub>2</sub> O <sub>5</sub>	0.2	0.4
SO <sub>3</sub>	0.6	0.1
CaO	2.6	0.2
ZrO <sub>2</sub>	0.2	0.1
Loss on ignition (950 °C)	2.2	2.0

The alkali activator was produced using NaOH pellets of analytical grade (~99%) and a sodium silicate solution composed of 26.5 wt.% SiO<sub>2</sub>, 10.6 wt.% Na<sub>2</sub>O and 62.9 wt.% H<sub>2</sub>O, supplied by Sigma Aldrich. The NaOH and the sodium silicate solution were blended to achieve the required overall molar ratio for each mix design.

155 **2.2. Sample preparation**

156 The geopolymer pastes were formulated with CKS/BA ratios of 75/25, 50/50, and 0/100, in each case with an  
 157 overall Na<sub>2</sub>O/Al<sub>2</sub>O<sub>3</sub> molar ratio of 1.0, and the dose of sodium silicate was adjusted to give an overall SiO<sub>2</sub>/Al<sub>2</sub>O<sub>3</sub>  
 158 molar ratio for each sample as specified in Table 2. The geopolymers were produced with a water/binder (w/b) ratio  
 159 of 0.40, where ‘binder’ here refers to the sum of the solid precursor and the anhydrous fraction of the alkali  
 160 activator. The pastes were mixed mechanically for 6 minutes and then cast into 20 mm cubic plastic moulds, and  
 161 then vibrated for one minute. The samples were cured at 50 °C for 24 h with a relative humidity (RH) of 90%, then  
 162 stored in a sealed plastic container at ~25 °C and RH>90% until testing. The mix designs of the geopolymers  
 163 produced are shown in Table .

164 Table 2- Mix designs and material constituents of the geopolymer samples produced.

Mix ID	CKS/BA ratio	Overall molar ratio			Material constituents (g)				
		Na <sub>2</sub> O/Al <sub>2</sub> O <sub>3</sub>	SiO <sub>2</sub> /Al <sub>2</sub> O <sub>3</sub>	water/binder	CKS	BA	Sodium silicate	NaOH	Extra water
100BA-5.9	0/100	1	5.9	0.40	0	100	0	15.9	40.6
100BA-7.0	0/100	1	7.0	0.40	0	100	46.7	8.8	15.3
50BA-4.0	50/50	1	4.0	0.40	50	50	0.0	22.9	49.2
50BA-4.5	50/50	1	4.5	0.40	50	50	32.0	18.6	32.1
50BA-5.0	50/50	1	5.0	0.40	50	50	64.5	14.1	14.7
25BA-3.5	75/25	1	3.5	0.40	75	25	0.0	20.1	48.0
25BA-4.0	75/25	1	4.0	0.40	75	25	24.5	16.7	34.9
25BA-4.5	75/25	1	4.5	0.40	75	25	52.9	12.8	19.7

165  
 166 Standard siliceous sand (ABNT NBR 7214:2015, [35]) with a fineness modulus of 2.5 and a maximum particle size  
 167 of 1.2 mm was used as the aggregate to prepare the mortars, which were formulated with a precursor:sand ratio of  
 168 1:3. The fresh mortar was cast in prismatic moulds of 40×40×160 mm, vibrated mechanically for 2 min and cured  
 169 under the same conditions described above for paste samples.

170 **2.3. Tests conducted**

171 *2.3.1 Pastes*

172 The chemical reaction of alkali-activation to form the geopolymer cements was monitored through isothermal  
 173 calorimetry using a TAM air microcalorimeter (TA Instruments) with a sensitivity of ± 20 μW. The temperature was  
 174 set to 50 °C, to match the temperature of the curing process. The precursors (BA and CKS) and the alkali activator  
 175 solution were pre-heated separately within the equipment for 45 min prior to the mixing. The mixtures were  
 176 prepared by mixing all constituents for 2 minutes inside the calorimeter. To enable a completely homogeneous fresh  
 177 mixture under these mixing conditions, the w/b ratio was adjusted to 0.50 for these tests; all other mix design  
 178 parameters were as shown in Table 2. The heat release was followed for 24 h.

179  
 180 The compressive strength was assessed for 5 cubic paste samples of 20 mm up to 450 days of curing, using a  
 181 universal testing machine (EMIC) with a displacement rate of 0.5 mm/min. For the tests after 3, 28, and 90 days of  
 182 curing, the samples used to determine compressive strength were collected after crushing, milled, washed with  
 183 isopropanol, filtered and then dried at ~50 °C for 20 min. The samples were stored in a vacuumed container until  
 184 microstructural characterisation. The reaction products were assessed through the following tests:

185  
 186 - X-ray diffraction (XRD), using a Siemens D5000 diffractometer with Cu Kα radiation, a scanning speed of 0.5  
 187 °/min and a step size of 0.020°, for a 2θ range between 7 and 70 degrees.

188 - Thermogravimetry with mass spectroscopy (TGA-MS), using a Perkin Elmer TGA 4000 coupled with a Hiden  
 189 Analytical mass spectrometer. The samples were heated to 1000 °C with a heating rate of 10 °C/min using alumina  
 190 crucibles, and nitrogen as a purge gas (100 mL/min). The mass spectrometer was programmed for the detection of  
 191 H<sub>2</sub>O and CO<sub>2</sub> signals.

192 - Fourier transform infrared (FTIR) spectroscopy, in a Perkin Elmer FTIR spectrometer using the KBr pellet  
 193 technique. The measurements were recorded in absorbance mode from 2500 to 400 cm<sup>-1</sup> with a resolution of 4 cm<sup>-1</sup>.

194 2.3.2 Mortars

195  
196 Key properties of mortars were evaluated to start the study of these precursors in an applicable material, and allow  
197 the analysis of properties associated with microstructure. The workability of fresh mortars was assessed with the  
198 testing protocol of the Brazilian standard NBR 13276 [36], and the compressive and flexural strength tests were  
199 performed following the procedure of NBR 13279 [37] after 1, 7 and 28 days. Water capillary suction was tested for  
200 samples after 28 days of curing based on the protocol NBR 15259 [38], in which water is allowed to pass into a  
201 dried sample through capillary suction, and the mass of the sample is monitored as a function of time.

202 **3. Results and discussion**

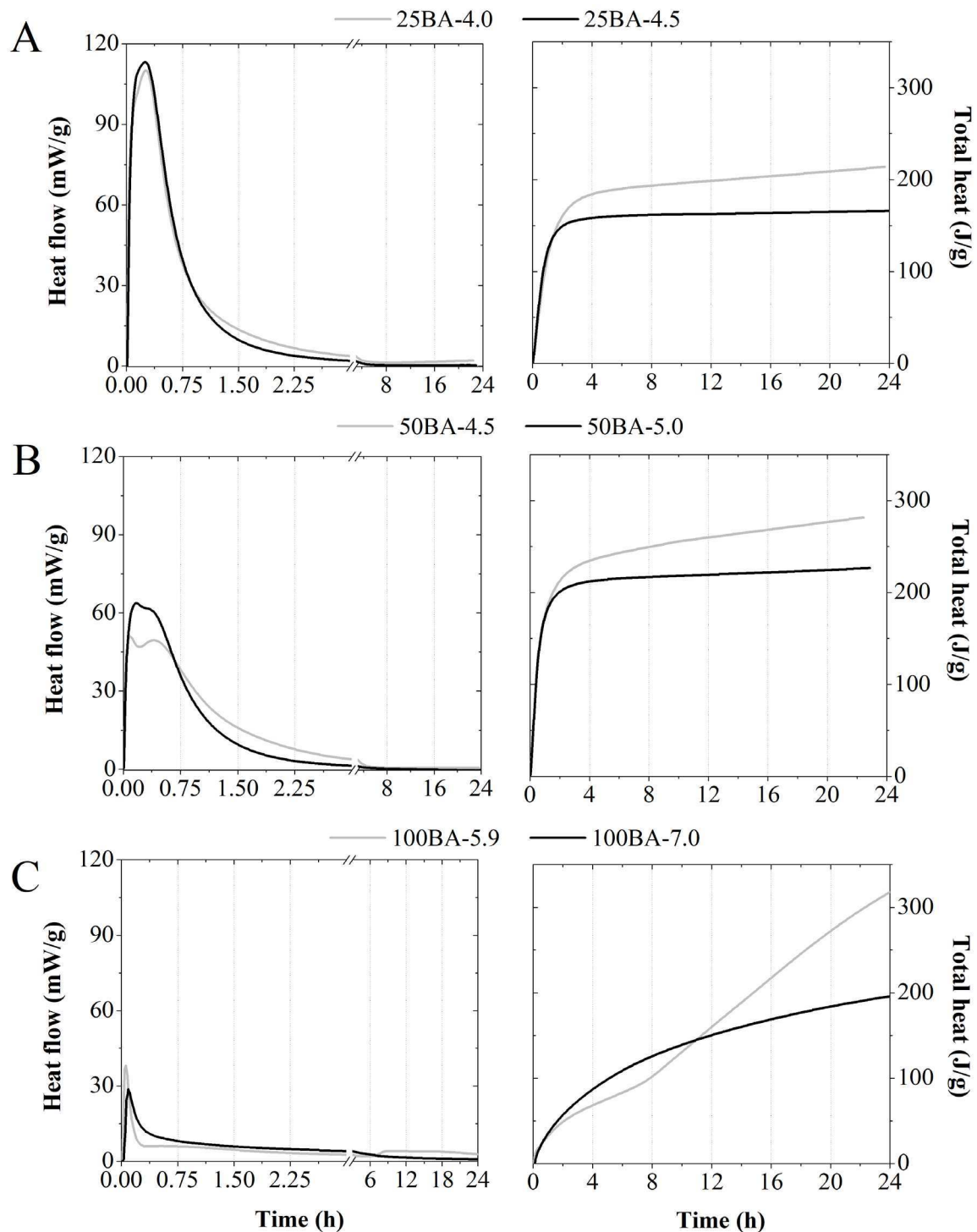
203 **3.1. Isothermal calorimetry**

204 Fig. 1 shows the heat released during geopolymerisation for the binary systems. The binary systems with a higher  
205 content of BA (50BA, in Fig. 1B) exhibit two peaks during the initial 45 min of reaction, and the content of sodium  
206 silicate has a strong effect on the heat released. Taking into account that internal mixing inside the calorimeter was  
207 used in this study, and the mix components were all thermally equilibrated prior to the start of the experiments, the  
208 data collected at this very early age can be considered more reliable than is the case when the more common  
209 external mixing protocol is used. At a lower content of soluble silicate (50BA-4.5) there are two distinguishable  
210 peaks located at 5 and 24 min, with a maximum intensity of 51 mW/g. The geopolymerisation process is exothermic  
211 due to the dissolution of the aluminosilicate precursors, oligomer formation, gelation and further gel reordering [39].  
212 In this sense, the first peak can be attributed to the dissolution of the precursors (BA/CKS) and release of silicate  
213 and aluminate monomers. The second and broader peak corresponds to the formation of aluminosilicate oligomers  
214 and the subsequent precipitation of an amorphous gel product (geopolymer) [40]. At a higher content of soluble  
215 silicate (50BA-5.0) the maximum rate of heat released increased to 63 mW/g and the second peak is less distinct.  
216 This indicates that the presence of a higher content of dissolved silicate species, which are supplied by the alkali  
217 activator, speed up the reaction due to faster polycondensation with the monomeric aluminate species released  
218 during the dissolution of the precursors. As an example, in Fig. 1B the 50BA-5.0 showed a total heat release of 166  
219 J/g at 24 h of reaction, which is ~20% lower than 50BA-4.5. Regardless of the CKS content, the total heat released  
220 is higher in systems with lower SiO<sub>2</sub>/Al<sub>2</sub>O<sub>3</sub> ratios, which indicates that the reaction is retarded and requires more  
221 time. This phenomenon was observed in a previous study using CKS as main precursor [35] and can be attributed to  
222 the aluminosilicate gel film formed, which envelops the dissolving particles and consequently reduces the rate of  
223 reaction. The increased content of SiO<sub>2</sub> was achieved through a higher content of bottom ash in the binary  
224 precursors system, as well as by the addition of soluble sodium silicate. Due to the lower reactivity of bottom ash,  
225 the increase in SiO<sub>2</sub> is more effective when the sodium silicate in the activator is increased.

226

227

228



229

230 **Fig. 1** Isothermal calorimetry data for the geopolymers as marked (sample IDs from Table 3) A. BA/CKS: 25/75; B.  
 231 BA/CKS:50/50 and C. BA:100/00. In each part, the left-hand plot shows the heat flow with the time axis expanded  
 232 by a factor of 10 in the early stages of the reaction, and the right-hand plot shows the cumulative heat release with a  
 233 linear time axis.

234

235 The presence of CKS, which has higher reactivity [34], modifies the kinetics of geopolymerisation so that a single  
 236 and more intense peak of heat release is identified at 15 min (Fig. 1B). Therefore, as the content of CKS increases  
 237 from 50 wt.% to 75 wt.% (for the systems 50BA and 25BA, respectively), a higher maximum of heat evolution is  
 238 reached, and earlier, and a narrower single exotherm is identified. Likewise, the cumulative heat released also  
 239 increased with higher contents of CKS. The higher content of  $\text{Al}_2\text{O}_3$  in the CKS increases the release of aluminate  
 240 monomers in the 25/75 BA/CKS blends. The higher heat release during the dissolution of the CKS can be attributed

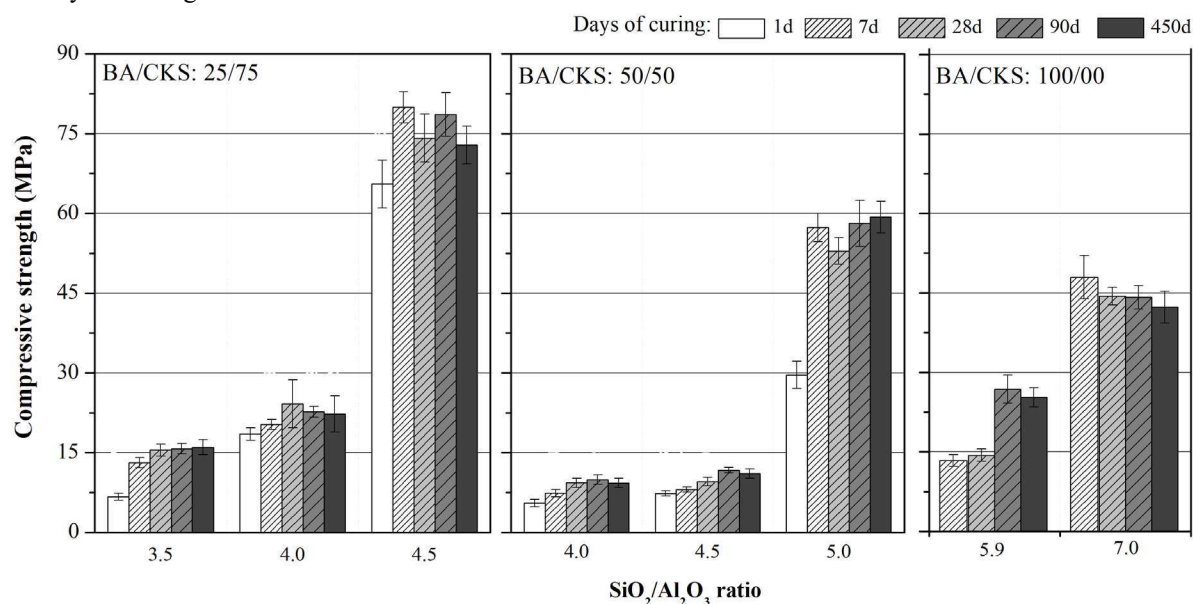


241 to the high specific surface area of the particles, as well as the presence of an amorphous and highly strained layer  
242 structure in kaolinitic clays after thermal treatment [40, 41].  
243

244 Under the activation conditions used, the dissolution of the BA is much lower than that of CKS due to the lower  
245 content of amorphous (or more reactive) phases; the crystalline phases present in the BA (see XRD analysis below)  
246 do not participate to a significant extent in the reactions [42]. The maximum heat released by the systems based on  
247 BA (Fig. 1C) is up to three times lower, when compared to the binary systems. The use of a blend of highly reactive  
248 and less reactive materials led to overlap between the dissolution and polycondensation processes [34].

### 249 3.2. Compressive strength of pastes

250 The mechanical performance of the materials produced is strongly influenced by the content of soluble silicate  
251 (which defines the overall  $\text{SiO}_2/\text{Al}_2\text{O}_3$  molar ratio for each precursor blend), as well as the BA/CKS ratio (Fig. 2).  
252 The bottom ash geopolymers system 100BA-5.9, which is activated by NaOH, presents an increasing compressive  
253 strength during the curing time, with a value of 26.7 MPa at 90 days of curing. The addition of sodium silicate, in  
254 100BA-7.0, provides higher mechanical performance (~44 MPa at 90 days). The blend 50BA-4.0, which has the  
255 lowest  $\text{SiO}_2/\text{Al}_2\text{O}_3$  molar ratio (and was produced with a NaOH-based activator) had a compressive strength lower  
256 than 10 MPa regardless of the duration of curing. However, this low mechanical performance can be improved by  
257 either using an alkali activator with higher content of soluble silicate, or by the inclusion of more CKS. In this sense,  
258 50BA-5.0, with a silicate activator giving an  $\text{SiO}_2/\text{Al}_2\text{O}_3$  molar ratio of 5.0, had a compressive strength up to 4 times  
259 higher than 50BA-4.0. Likewise, the adjustment of the BA/CKS ratio in the precursor to 25/75 (higher content of  
260 CKS) with an  $\text{SiO}_2/\text{Al}_2\text{O}_3$  molar ratio of 4.0 (25BA-4.0) gave a compressive strength up to 2.8 times higher than that  
261 of 50BA-4.0. Similar behavior is also identified in the pastes with an  $\text{SiO}_2/\text{Al}_2\text{O}_3$  molar ratio of 4.5; 25BA-4.5 had a  
262 compressive strength up to four times higher than 50BA-4.5. According to previous studies, the CKS-based systems  
263 produced using NaOH as activator exhibited compressive strengths lower than 20 MPa even after 90 days of curing  
264 [34]. This value is considerably lower than for the corresponding BA-based systems, whose compressive strength at  
265 90 days of curing is close to 30 MPa.

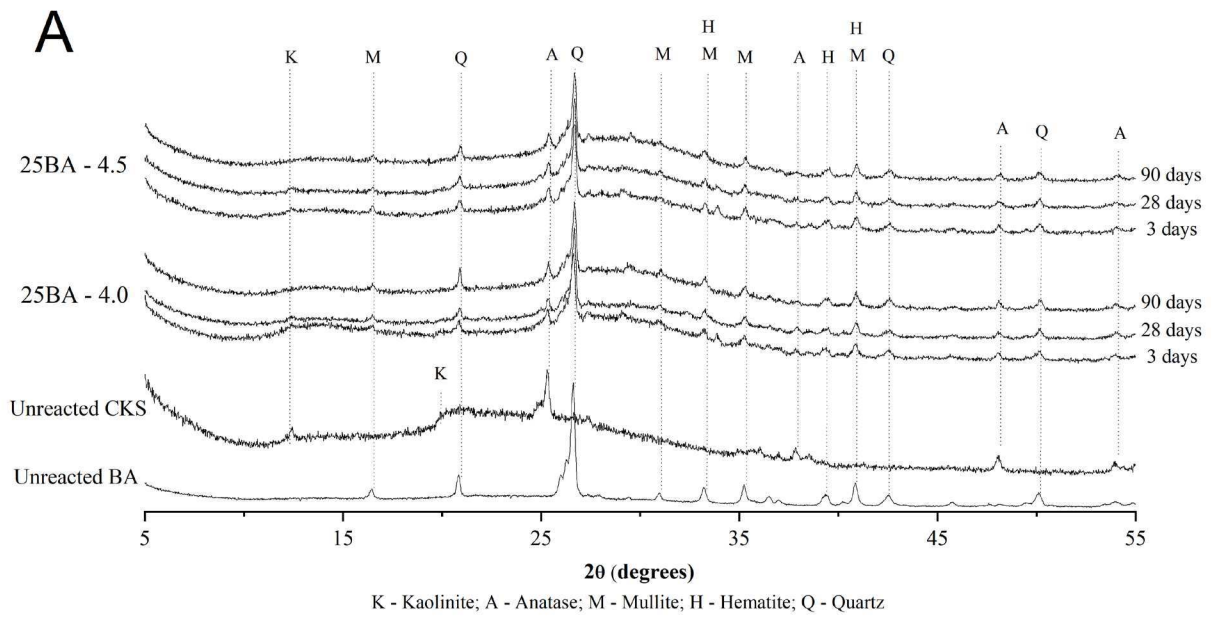


266 **Fig. 2** Compressive strength of the geopolymers with different BA/CKS ratios as marked. Errors bars indicate  
267 standard deviation.  
268

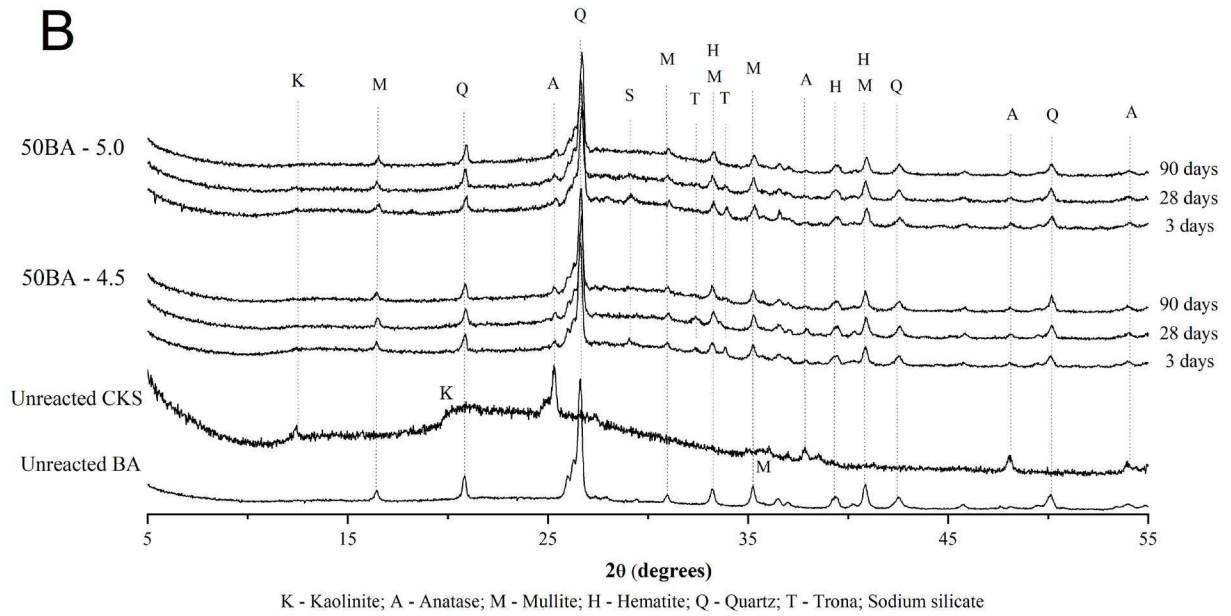
269 From these data, there does not exist a direct and proportional relation between the total heat released and the  
270 compressive strength. The higher values of total heat do not indicate the formation of stronger and more cross-  
271 linked microstructure. For example, although 25BA-4.5 showed lower total heat release when compared with 25BA-  
272 4.0 (Fig. 1a), it also had the highest compressive strength after 1 days of curing. The pastes that achieved high  
273 compressive strength (> 25 MPa) also showed a significant standard deviation in the results, which makes unclear  
274 the behavior between different durations of curing.  
275

276 **3.3. Binder characterisation**

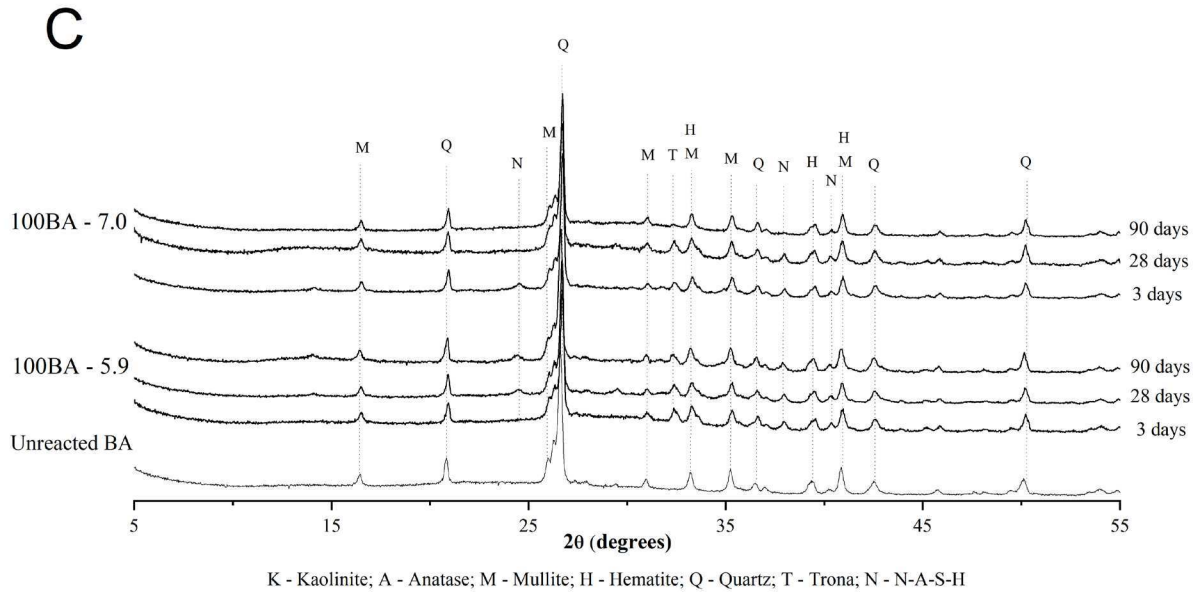
277 Fig. 3 shows the X-ray diffractograms of the unreacted precursors (BA and CKS) and the geopolymers after 3, 28  
278 and 90 days of curing. The crystalline phases present in the BA and CKS, including mullite ( $\text{Al}_6\text{Si}_2\text{O}_{13}$ , Pattern  
279 Diffraction File, PDF# 01-083-1881), hematite ( $\text{Fe}_2\text{O}_3$ , PDF# 01-079-0007), quartz ( $\text{SiO}_2$ , PDF# 01-088-2302), and  
280 anatase ( $\text{TiO}_2$ , PDF# 00-021-1272) are identified in all samples regardless the synthesis conditions or age of curing.  
281 The presence of well-defined peaks and the lower intensity of the amorphous hump in the BA corroborates its lower  
282 reactivity, which is also identified through the lower mechanical performance and lower heat release observed for  
283 the geopolymer produced with this precursor. On the other hand, the CKS shows an intense amorphous hump, with  
284 few traces of the remaining kaolinite ( $\text{Al}_2\text{Si}_2\text{O}_5(\text{OH})_4$ , PDF# 01-078-2109). The pronounced amorphous hump  
285 shown by the CKS in the  $2\theta$  range between 20 and  $30^\circ$  decreases and shifts to higher angles after alkali-  
286 activation, which can be attributed to the formation of aluminosilicate gels [34, 43]. The X-ray diffractograms of all  
287 pastes studied are quite similar, regardless of the activator composition and BA/CKS ratio, and no crystalline zeolite  
288 phases were identified as reaction products, even after 90 days of curing. The patterns for the systems with a  
289 BA/CKS ratio of 50/50 showed a higher amorphous hump between 25 and  $35^\circ$   $2\theta$ , related to the gels which can be  
290 related to the higher heat released during the first 24 hours due to a more extended formation of the geopolymeric  
291 gel, which is also consistent with the mechanical strength previously reported. Sodium carbonate ( $\text{Na}_2\text{CO}_3$ ; PDF#  
292 01-086-0312) was identified in the sample 50BA-4.5 due to reaction of the sodium-rich pore solution with the  
293 atmospheric  $\text{CO}_2$  during either curing or handling.



294



295



296

297 **Fig. 3** X-ray diffractograms of the unreacted precursors, and of the geopolymers at different ages of curing. A.

298

BA/CKS: 25/75; B. BA/CKS:50/50; and C. BA/CKS:100/00.

299

300 Fig 4. to Fig. 6 show the thermogravimetric analysis and accompanying MS spectra for masses of CO<sub>2</sub> (40 g/mol)  
 301 and H<sub>2</sub>O (18 g/mol), for the geopolymers with different BA/CKS ratios up to 90 days of curing. The DTG curves  
 302 each exhibit a strong peak between 25-250 °C, which is attributed to the loss of trapped water from the gel pore  
 303 structure, and the water physically bound to the reaction products. There are no significant differences in the  
 304 temperature of the main peak in the DTG curves among the samples assessed, which indicates that these water  
 305 environments are similar in all samples. The geopolymers with a BA/CKS ratio of 25/75 (Fig. 4) have a lower total  
 306 mass loss when compared with the ratio 50/50 (Fig. 5), which is attributed to a more extensive formation of reaction  
 307 products. The mass spectroscopy also shows the release of water, whose highest signal was detected between 105  
 308 and 120 °C. At higher temperature (400-500 °C) the water present as hydroxyl groups in the aluminosilicate  
 309 framework is released [44]. These results confirm that most of the water in the geopolymeric system is present as  
 310 free or adsorbed water, with little chemically bound as hydroxyl groups.

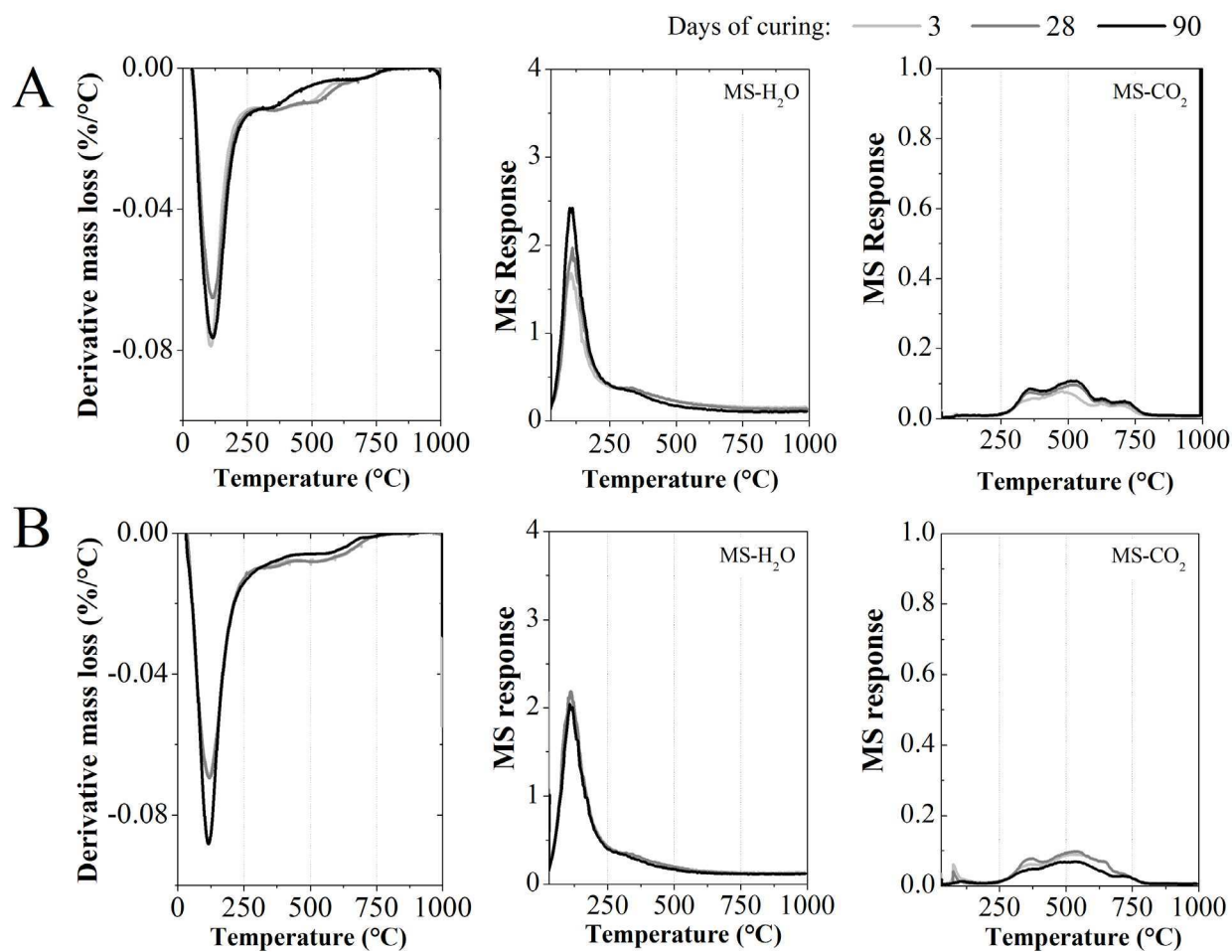
311

312 The water released by the geopolymer with a BA/CKS ratio of 25/75 and an SiO<sub>2</sub>/Al<sub>2</sub>O<sub>3</sub> molar ratio of 4.5 was  
 313 lower when compared to the corresponding systems produced with a higher content of soluble silicates (SiO<sub>2</sub>/Al<sub>2</sub>O<sub>3</sub>  
 314 molar ratio of 5.0), which can be linked to differences in the quantity of gel formed. These results are consistent  
 315 with the lower mechanical performance exhibited by 50BA-4.5 compared to 50BA-5.0. For the systems with a  
 316 BA/CKS ratio of 25/75 (Fig. 6), no significant differences in the total mass loss were identified regardless of the  
 317 SiO<sub>2</sub>/Al<sub>2</sub>O<sub>3</sub> ratio, despite the very notable difference in strength between 25BA-4.5 and the other pastes at this  
 318 BA/CKS ratio (Figure 2).

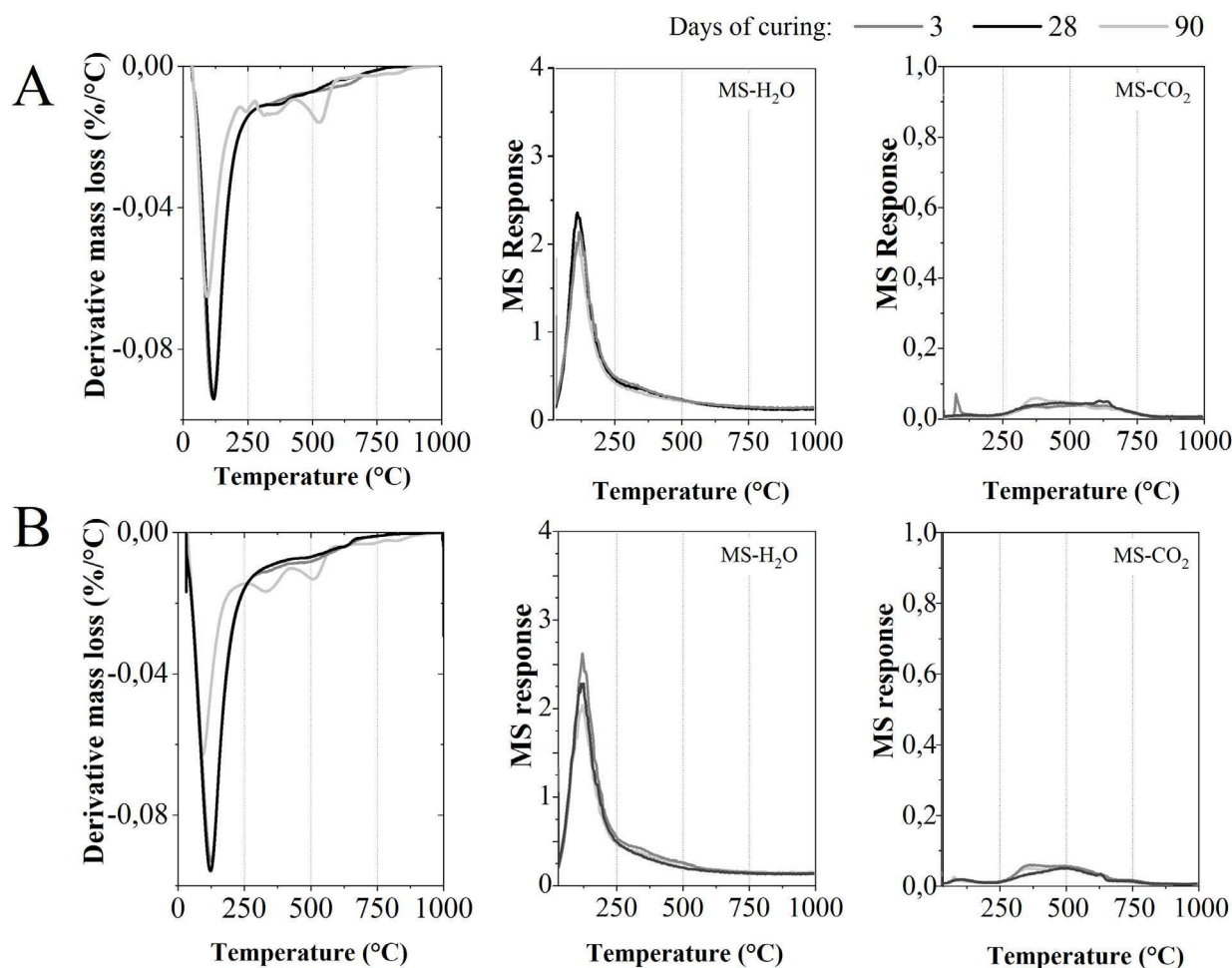
319

320

321



322  
 323 **Fig 4** Differential thermogravimetric curves (DTG), and water and carbon dioxide mass spectroscopy (MS)  
 324 for the geopolymers produced with a BA/CKS ratio of 25/75 at different SiO<sub>2</sub>/Al<sub>2</sub>O<sub>3</sub> molar ratios: A, 4.0; and B, 4.5.  
 325

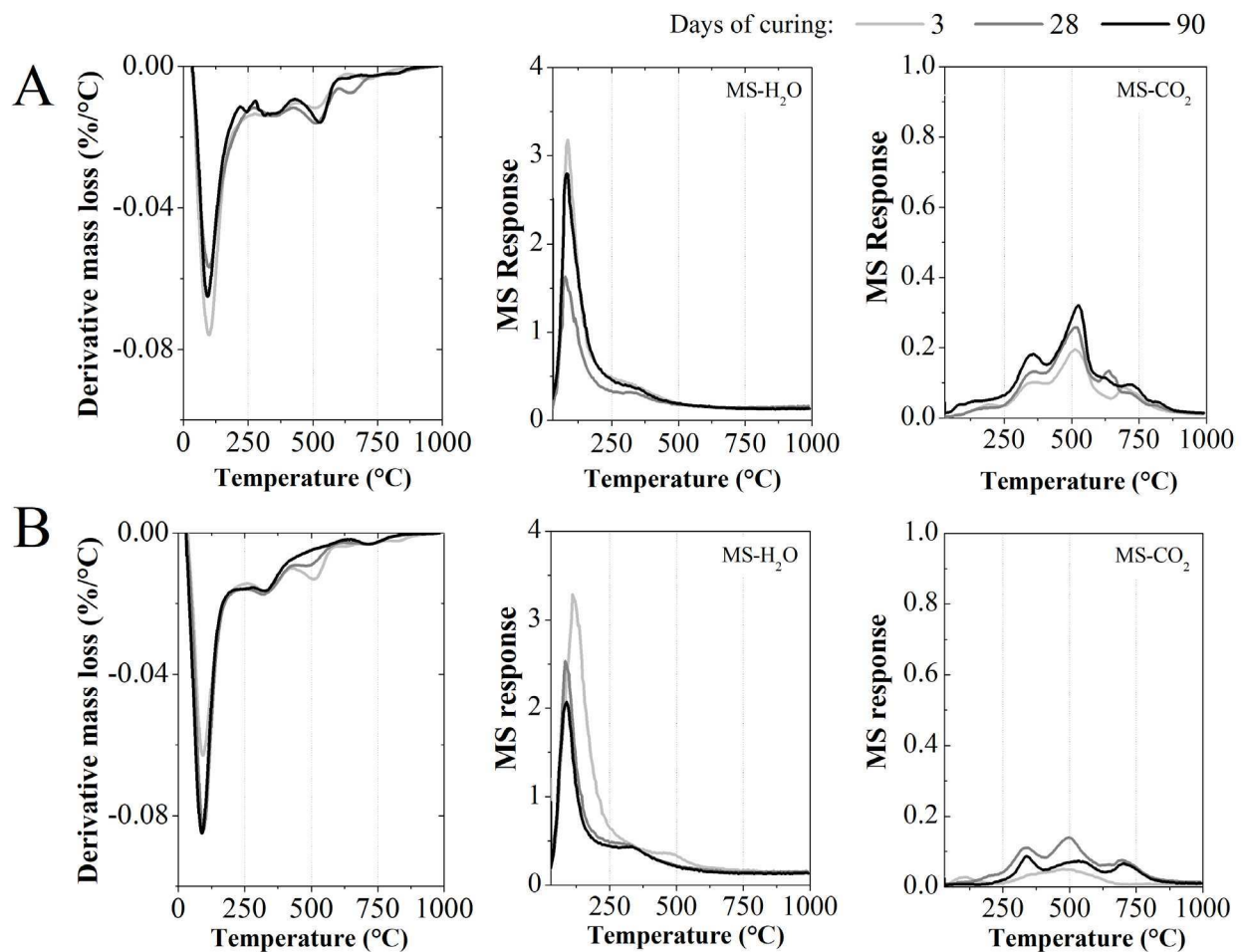


326

327 **Fig. 5** Differential thermogravimetric curves (DTG), and water and carbon dioxide mass spectroscopy (MS) results  
 328 for the geopolymers produced with a BA/CKS ratio of 50/50 at different  $\text{SiO}_2/\text{Al}_2\text{O}_3$  molar ratios: A, 4.5; and B, 5.0.

329  
 330 The release of  $\text{CO}_2$  detected by the mass spectroscopy showed two stages, the first one with a peak between 70 and  
 331 90 °C, followed by a broader and more intense signal located between 350 and 700 °C. The signal identified at  
 332 lower temperatures can be attributed to the thermal conversion of minor alkali carbonates formed due to carbonation  
 333 of the sample during handling and storage. The second signal can be attributed to the thermal decomposition of  
 334 different calcium carbonates-containing products with low crystallinity (not identified in the X-ray diffractograms).  
 335 The content of carbonates is slightly higher as the content of BA is increased, as this is the precursor that supplied  
 336 Ca into the system, and can also indicate an excessive amount of activator that can lead to the carbonation of the  
 337  $\text{Na}^+$ . These results are also consistent with the peak with a low intensity identified between 600 and 750 °C in the  
 338 DTG curves.

339  
 340



341  
 342 **Fig. 6** Differential thermogravimetric curves (DTG), and water and carbon dioxide mass spectroscopy (MS) results  
 343 for the geopolymers produced with a BA/CKS ratio of 100/0 at different SiO<sub>2</sub>/Al<sub>2</sub>O<sub>3</sub> molar ratios: A, 5.9; and B, 7.0.  
 344

### 345 3.4. Mortars

346 The paste mix designs of the geopolymers with BA/CKS ratios of 50/50 and 25/75 with SiO<sub>2</sub>/Al<sub>2</sub>O<sub>3</sub> molar ratios of  
 347 5.0 and 4.5, respectively, which showed the highest compressive strength results in the paste mixtures (Fig. 2) were  
 348 used for the production of mortars. Fig. 7 shows the workability of the fresh mixtures, and the compressive and  
 349 flexural strengths of the geopolymeric mortars assessed after 3, 7 and 28 days of curing. The 50BA-5.0 mortar  
 350 exhibited a higher workability than 25BA-4.5, which is attributed to the lower content of CKS. As observed in a  
 351 previous paper [35], the morphology of CKS is a plate-like particle structure with high surface area and high  
 352 reactivity, and these properties tend to increase the water demand [45]. The high content of soluble silicate in the  
 353 alkali activator also reduced the workability of the fresh mixture, which is related to the higher viscosity of alkali  
 354 activator solutions with high SiO<sub>2</sub>/Na<sub>2</sub>O molar ratio [46].  
 355

356 The compressive strengths of the mortars are consistent with the results presented above for pastes, where 25BA-4.5  
 357 exhibited the highest mechanical performance. After 28 days of curing both mortars showed compressive strength  
 358 values higher than 50 MPa, which elucidates the high degree of valorisation that is achieved for the waste materials  
 359 here. The mortars also showed a clear evolution in the strength development, so that at 28 days the compressive  
 360 strength of these mortars are up to ~40% higher than the corresponding systems at earlier ages. In this sense, the  
 361 inclusion of the sand as a fine aggregate removed the loss of compressive strength due to shrinkage-related  
 362 processes that was identified in the results in pastes (Fig. 2). Sand particles act as a reinforcement which also  
 363 provides dimensional stability [47]. However, it is not clear why the flexural strengths of both mortars show the  
 364 opposite behavior and appear to regress from 7 to 28 days.  
 365  
 366  
 367

368  
369

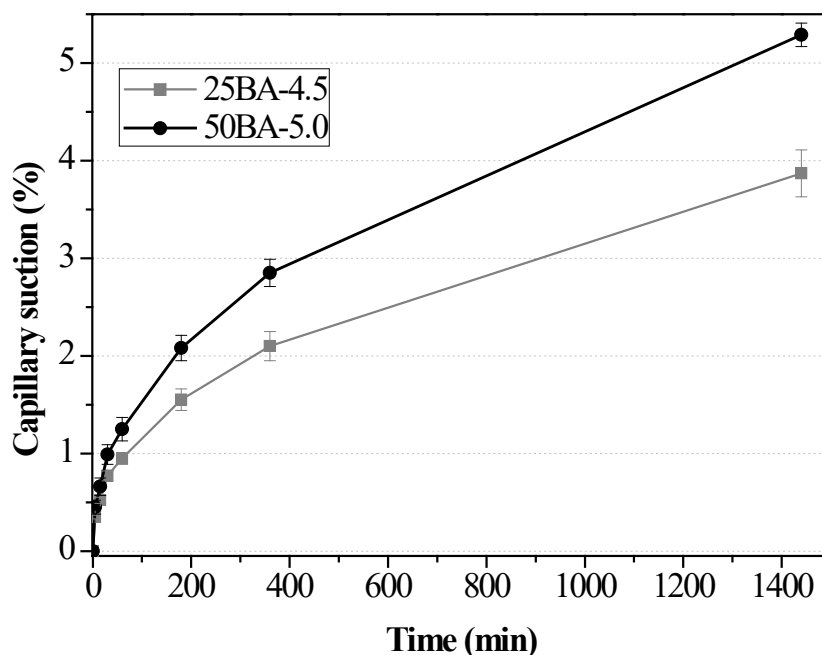
370 Table 2 Compressive strength and flexural for the geopolymers mortars

Mortar ID	Flow of fresh mortars, NBR 13276 [36] (mm)	Age (days)	Compressive strength		Flexural strength	
			MPa	SD	MPa	SD
25BA-4.5	174	7	49.9	7.1	9.3	0.5
		28	58.3	7.3	7.2	0.7
50BA-5.0	182	7	34.8	3.5	6.5	0.2
		28	47.6	6.6	6.7	0.9

SD: Standard deviation among 6 samples

371  
372  
373  
374  
375  
376  
377  
378  
379  
380  
381  
382

Capillary sorptivity curves obtained for the mortars after 28 days of curing are shown in Fig. 7. The low sorptivity, associated with a low pore volume and a refined pore structure, is desirable from a durability point of view. According to NBR 15259:2005 [38], the kinetics of the water sorption can be described by a capillary absorption coefficient calculated from the values obtained after 10 and 90 min. Following this calculation procedure, mortars 25BA-4.5 and 50BA-5.0 had capillary coefficients of 3.39 and 4.45 g/dm<sup>2</sup>·min<sup>1/2</sup>, respectively. The water absorption after 24 h is similar between the two mortars, but the relative rates of the water sorption in the two samples indicate a denser pore structure with a higher tortuosity for 25BA-4.5, which is consistent with the higher mechanical strength of this mortar.



383

384 Fig. 7 Capillary sorptivity of geopolymer mortars after 28 days of curing.

385 The results of compressive strength and porosity determination are clearly related to microstructural properties. The  
386 higher compressive strength is also observed in the systems produced with higher alkali activator dose based on  
387 sodium silicate, which is aligned with the behavior identified in the pastes. The porosity is reduced by the presence  
388 of sodium silicate in the alkali activator, which is also associated with the higher amount of gel formed during the  
389 geopolymerisation, where the most reactive blend of precursors shows a lower water absorption when compared to  
390 the less reactive blend precursor system. These results indicate that these precursors (CKS and BA) are promising  
391 materials to be used in geopolymers at large scale.

392



#### 393 4. Conclusions

394 Coal bottom ash (BA) and calcined kaolin sludge (CKS) can be valorised as precursors for blended geopolymer  
395 pastes and mortars. The partial replacement of BA by CKS increases the average reactivity of the precursor blend,  
396 and thus also the heat released during geopolymerisation and improve the workability when using the same amount  
397 of water. The inclusion of an optimum content of silicate soluble increases the compressive strength very  
398 significantly, and materials with attractive mechanical performance can be obtained across a wide range of BA/CKS  
399 ratios. The results reported in the present study elucidate that the presence of soluble silicates in the alkali activator,  
400 and the inclusion of a higher content of a precursor with high reactivity, play a significant role in determining the  
401 mechanical performance of a geopolymer material. The disordered aluminosilicate gel structure that gives strength  
402 to the binders can also be tailored to give relatively low capillary uptake coefficients, and the paste mix designs  
403 generated in this work can be scaled to give mortars with desirable mechanical performance. The results also  
404 elucidate that the understanding of synthesis optimisation through the adjustment of the alkali activator composition  
405 and dosage is a useful way to increase the potential valorisation of those industrial wastes that exhibit lower  
406 reactivity. Therefore, the geopolymerisation of some industrial wastes can be considered an interesting pathway for  
407 their reuse, and more detailed studies (such as real environmental impact, durability, application and cost) are  
408 required for the large-scale inclusion of this new material within the industry.

#### 409 Acknowledgements

410 The participation of SAB and JLP was sponsored by the Brazilian National Council for Scientific and Technological  
411 Development (CNPq) through its PVE program, and the Royal Academy of Engineering through a Newton Fund  
412 Research Collaboration Fellowship between Brazil and the UK. The participation of EDR and APK received  
413 funding from CNPq through grant numbers PQ 303753/2017-0 and 305530/2017-8, respectively. The authors  
414 also acknowledge the Laboratory of Ceramics (LACER) and Building Innovation Research Unit (NORIE) at  
415 Federal University of Rio Grande do Sul (UFRGS) and the Department of Materials Science and Engineering at the  
416 University of Sheffield.

#### 417 References

- 418 1. United Nations: The Millennium Development Goals Report 2015. , New York, US (2015)
- 419 2. World Coal Association: Coal Facts 2014. , London, U.K. (2014)
- 420 3. Heidrich, C., Feuerborn, H.J., Weir, A.: Coal combustion products: A global perspective. In: 2013 World of  
421 Coal Ash (WOCA) Conference. pp. 1–16. , Lexington, KY, United States (2013)
- 422 4. Freitas, A.P.P., Schneider, I.A.H., Schwartzbold, A.: Biosorption of heavy metals by algal communities in  
423 water streams affected by the acid mine drainage in the coal-mining region of Santa Catarina state, Brazil.  
424 *Miner. Eng.* 24, 1215–1218 (2011). doi:10.1016/j.mineng.2011.04.013
- 425 5. Lukacs, H., Ortolano, L.: West Virginia has not directed sufficient resources to treat acid mine drainage  
426 effectively. *Extr. Ind. Soc.* 2, 194–197 (2015). doi:10.1016/j.exis.2014.12.002
- 427 6. Silva, L.F.O., Fdez-Ortiz de Vallejuelo, S., Martinez-Arkarazo, I., Castro, K., Oliveira, M.L.S., Sampaio,  
428 C.H., de Brum, I.A.S., de Leão, F.B., Taffarel, S.R., Madariaga, J.M.: Study of environmental pollution and  
429 mineralogical characterization of sediment rivers from Brazilian coal mining acid drainage. *Sci. Total*  
430 *Environ.* 447, 169–178 (2013). doi:10.1016/j.scitotenv.2012.12.013
- 431 7. Anawar, H.M.: Sustainable rehabilitation of mining waste and acid mine drainage using geochemistry, mine  
432 type, mineralogy, texture, ore extraction and climate knowledge. *J. Environ. Manage.* 158, 111–121 (2015).  
433 doi:10.1016/j.jenvman.2015.04.045
- 434 8. ecoba European Coal Combustion Products Association: Production and utilisation of CCPs in 2010 in  
435 Europe (EU15)
- 436 9. ACAA American Coal Ash Association: 2012 Coal combustion product (CCP) production & use survey  
437 report
- 438 10. Asokan, P., Saxena, M., Asolekar, S.R.: Coal combustion residues—environmental implications and  
439 recycling potentials. *Resour. Conserv. Recycl.* 43, 239–262 (2005). doi:10.1016/j.resconrec.2004.06.003
- 440 11. Sajwan, K.S., Punshon, T., Seaman, J.C.: Production of coal combustion products and their potential uses.  
441 In: Sajwan, K., Twardowska, I., Punshon, T., and Alva, A. (eds.) *Coal Combustion Byproducts and*  
442 *Environmental Issues SE - 1*. pp. 3–9. Springer New York (2006)
- 443 12. 40 CFR Parts 257 and 261. Hazardous and solid waste management system; disposal of coal combustion  
444 residuals from electric utilities; Final Rule. , US (2015)
- 445 13. Cheriaf, M., Rocha, J.C., Péra, J.: Pozzolanic properties of pulverized coal combustion bottom ash. *Cem.*  
446 *Concr. Res.* 29, 1387–1391 (1999)
- 447 14. An, E.-M., Cho, S.-B., Lee, S.-J., Miyauchi, H., Kim, G.-Y.: Compressive strength properties of geopolymer

- 448 using power plant bottom ash and NaOH activator. *Korean J. Mater. Res.* 22, 71–77 (2012).  
 449 doi:10.3740/MRSK.2012.22.2.71
- 450 15. Chindaprasirt, P., Jaturapitakkul, C., Chalee, W., Rattanasak, U.: Comparative study on the characteristics  
 451 of fly ash and bottom ash geopolymers. *Waste Manag.* 29, 539–43 (2009).  
 452 doi:10.1016/j.wasman.2008.06.023
- 453 16. Chotetanorm, C., Chindaprasirt, P.: High-calcium bottom ash geopolymer: sorptivity, pore size, and  
 454 resistance to sodium sulfate attack. *J. Mater. Civil Eng.* 25, 105–111 (2012). doi:10.1061/(ASCE)MT.1943-  
 455 5533
- 456 17. Kim, S.H., Ryu, G.S., Koh, K.T., Kang, S.T., Lee, J.H.: Effect on the alkali-activator mixing ratio of  
 457 geopolymer mortar using bottom ash. *Key Eng. Mater.* 488–489, 411–414 (2011).  
 458 doi:10.4028/www.scientific.net/KEM.488-489.411
- 459 18. Sathonsaowaphak, A., Chindaprasirt, P., Pimraksa, K.: Workability and strength of lignite bottom ash  
 460 geopolymer mortar. *J. Hazard. Mater.* 168, 44–50 (2009). doi:10.1016/j.jhazmat.2009.01.120
- 461 19. Van Deventer, J.S.J., Provis, J.L., Duxson, P.: Technical and commercial progress in the adoption of  
 462 geopolymer cement. *Miner. Eng.* 29, 89–104 (2012). doi:10.1016/j.mineng.2011.09.009
- 463 20. Provis, J.L., van Deventer, J.S.J. (eds.): *Geopolymers. Structure, processing, properties and industrial*  
 464 *applications.* Woodhead Publishing, Cambridge (2009)
- 465 21. Boonserm, K., Sata, V., Pimraksa, K., Chindaprasirt, P.: Improved geopolymerization of bottom ash by  
 466 incorporating fly ash and using waste gypsum as additive. *Cem. Concr. Compos.* 34, 819–824 (2012).  
 467 doi:10.1016/j.cemconcomp.2012.04.001
- 468 22. Longhi, M.A., Kirchheim, A.P.: Álcali-ativação de lodo de caulim calcinado e cinza pesada com ativadores  
 469 convencionais e silicato de sódio alternativo, (2015)
- 470 23. Sundstron, M.G.: Caracterização e avaliação das cinzas da combustão de carvão mineral geradas na região  
 471 do baixo jacui. Master Thesis, Unilasalle, Canoas, Brazil, (2012)
- 472 24. Rohde, G.M., Zwonok, O., Chies, F., Silva, N.I., Oleg, Chies, Silva: *Cinzas de carvão fóssil no Brasil.*  
 473 *Cientec publishing, Porto Alegre* (2006)
- 474 25. Departamento Nacional de Produção Mineral: *Sumário Mineral 2014.* , Brasilia (2014)
- 475 26. Barata, M.S., Angélica, R.S.: Caracterização dos resíduos cauliniticos das indústrias de mineração de caulim  
 476 da amazônia como matéria-prima para produção de pozolanas de alta reatividade ( *Characterization of*  
 477 *kaolin wastes from kaolin mining industry.* *Cerâmica.* 58, 36–42 (2012)
- 478 27. Associação Brasileira de Normas Técnicas: ABNT NBR10004/2004: *Classificação de Resíduos Sólidos*  
 479 *(Solid waste - Classification).* (2004)
- 480 28. Murray, H.H., Alves, C.A., Bastos, C.H.: Mining, processing and applications of the Capim Basin kaolin,  
 481 Brazil. *Clay Miner.* 42, 145–151 (2007). doi:10.1180/claymin.2007.042.2.01
- 482 29. Prasad, M.S., Reid, K.J., Murray, H.H.: Kaolin: processing, properties and applications. *Appl. Clay Sci.* 6,  
 483 87–119 (1991)
- 484 30. Frías, M., la Villa, R.V., Rojas, M.S., Medina, C., Juan Valdés, A.: Scientific aspects of kaolinite based coal  
 485 mining wastes in pozzolan/Ca(OH)<sub>2</sub> system. *J. Am. Ceram. Soc.* 95, 386–391 (2012). doi:10.1111/j.1551-  
 486 2916.2011.04985.x
- 487 31. Dias, S.L., Guimarães, I.O., Figueiredo, S.S., Bezerra, I.M.T., Ferreira, H.C., Neves, G.A.: Influence of  
 488 firing temperature on the pozzolanic activity of kaolin wastes. In: *Materials Science Forum.* pp. 675–680  
 489 (2012)
- 490 32. Barata, M.S., Angélica, R.S.: Pozzolanic activity of kaolin wastes from kaolin mining industry from the  
 491 amazon region. *Matéria.* 16, 795–810 (2011)
- 492 33. Longhi, M., Gaedke, F., Rodríguez, E., Passuello, A., Kirchheim, A.P., Bernal, S., Provis, J.: Geopolymers  
 493 based on calcined kaolin sludge/ bottom ash blends and an alternative sodium silicate activator. In: *34th*  
 494 *Cement and Concrete Science Conference.* p. 182, Sheffield. United Kingdom (2014)
- 495 34. Longhi, M.A., Rodríguez, E.D., Bernal, S.A., Provis, J.L., Kirchheim, A.P.: Valorisation of a kaolin mining  
 496 waste for the production of geopolymers. *J. Clean. Prod.* 115, (2016). doi:10.1016/j.jclepro.2015.12.011
- 497 35. Associação Brasileira de Normas Técnicas: ABNT NBR 7214:2012: *Areia normal para ensaio de cimento -*  
 498 *Especificação (Standard sand for cement test - Specification),* (2012)
- 499 36. Associação Brasileira de Normas Técnicas: ABNT NBR 13276: *Argamassa para assentamento e*  
 500 *revestimento de paredes e tetos - Preparo da mistura e determinação do índice de consistência. (Mortars*  
 501 *applied on walls and ceilings - Preparation of mortar for unit masonry and rendering with standard consis,*  
 502 *(2005)*
- 503 37. Associação Brasileira de Normas Técnicas: ABNT NBR 13279:2005: *Argamassa para assentamento e*  
 504 *revestimento de paredes e tetos - Determinação da resistência à tração na flexão e à compressão (Mortars*  
 505 *applied on walls and ceilings - Determination of the flexural and the compressive strength in the h.* (2005)
- 506 38. Associação Brasileira de Normas Técnicas: ABNT NBR 15259:2005: *Argamassa para assentamento e*  
 507 *revestimento de paredes e tetos - Determinação da absorção de água por capilaridade e do coeficiente de*

- 508 capilaridade (Mortars applied on walls and ceilings - Determination of water absorption coefficient . (2005)  
509 39. Provis, J.L., Duxson, P., Van Deventer, J.S.J., Lukey, G.C.: The role of mathematical modelling and gel  
510 chemistry in advancing geopolymer technology. *Chem. Eng. Res. Des.* 83, 853–860 (2005).  
511 doi:10.1205/cherd.04329
- 512 40. Provis, J.L., van Deventer, J.S.J.: Geopolymerisation kinetics. 2. Reaction kinetic modelling. *Chem. Eng.*  
513 *Sci.* 62, 2318–2329 (2007). doi:10.1016/j.ces.2007.01.028
- 514 41. Zhang, Z., Wang, H., Zhu, Y., Reid, A., Provis, J.L., Bullen, F.: Using fly ash to partially substitute  
515 metakaolin in geopolymer synthesis. *Appl. Clay Sci.* 88–89, 194–201 (2014).  
516 doi:10.1016/j.clay.2013.12.025
- 517 42. Fernández-Jimenez, A., de la Torre, A.G., Palomo, A., López-Olmo, G., Alonso, M.M., Aranda, M.A.G.:  
518 Quantitative determination of phases in the alkali activation of fly ash. Part I. Potential ash reactivity. *Fuel.*  
519 85, 625–634 (2006)
- 520 43. Zhang, Z., Wang, H., Provis, J.L., Bullen, F., Reid, A., Zhu, Y.: Quantitative kinetic and structural analysis  
521 of geopolymers. Part 1. The activation of metakaolin with sodium hydroxide. *Thermochim. Acta.* 539, 23–  
522 33 (2012). doi:10.1016/j.tca.2012.03.021
- 523 44. Duxson, P., Lukey, G.C., Deventer, J.S.J.: Physical evolution of Na-geopolymer derived from metakaolin  
524 up to 1000 °C. *J. Mater. Sci.* 42, 3044–3054 (2007). doi:10.1007/s10853-006-0535-4
- 525 45. Provis, J.L., Duxson, P., van Deventer, J.S.J.: The role of particle technology in developing sustainable  
526 construction materials. *Adv. Powder Technol.* 21, 2–7 (2010). doi:10.1016/j.appt.2009.10.006
- 527 46. Provis, J.L.: Activating solution chemistry for geopolymers. In: Provis, J.L. and van Deventer, J.S.J. (eds.)  
528 *Geopolymers: Structure, processing, properties and industrial applications.* pp. 50–66. Woodhead,  
529 Cambridge (2009)
- 530 47. Maruyama, I., Sasano, H., Lin, M.: Impact of aggregate properties on the development of shrinkage-induced  
531 cracking in concrete under restraint conditions. *Cem. Concr. Res.* 85, 82–101 (2016).  
532 doi:10.1016/j.cemconres.2016.04.004  
533